Theoret. Chim. Acta (Berl.) 44, 323–339 (1977)

THEORETICA CHIMICA ACTA

Molecular Orbital Studies of Hydrogen Bonds

X. The Ground and Low-Lying Excited States of Formic Acid Dimer*

Suehiro Iwata** and Keiji Morokuma

Department of Chemistry, The University of Rochester, Rochester, N.Y. 14627, USA

The ground state, the lowest singlet and triplet n-π^* states, and the lowest triplet π-π^* state of the formic acid monomer and dimer are studied with the *ab initio* molecular orbital theory. The two-configuration electron-hole potential method is used for calculations of excited states of dimers. The potential energy curves for the symmetrical simultaneous movement of two bridging protons are studied for all of the states. The barrier of the proton transfer in the ground state is found to be the smallest of the states studied. The association energy is analyzed in terms of various components.

Key words: Formic acid dimer – Hydrogen bond

1. Introduction

In recent years the *ab initio* SCF MO method has been extensively applied to studies of hydrogen-bonding interaction in the ground state [1-3]. The results were, in general, successful in predicting hydrogen-bonding energies and geometries of complexes. In the present series of papers [4-6] we first extended our studies to hydrogen bonding in excited states. The extension was made possible by developing a new approximate method for the calculation of excited states, the electron-hole potential (EHP) method [7, 8]. The method is simple and systematic, and the wave function is easy to handle, so that the interaction energy decomposition analysis, which has previously been proposed for the ground state [1a], can be extended to the excited state interaction.

In the present paper the formic acid monomer and dimer are studied. The n-π^* triplet and singlet, π-π^* triplet states, as well as the ground state, of the dimer and monomer are investigated. One of the interesting aspects of this dimer is its biological implication. The dimer is bridged by two hydrogen bonds, and therefore it may serve as a model of the proton exchange between base pairs in nucleic acids. Using a semi-empirical SCF method, Rein and Harris [9] calculated the potential energy curve for the proton transfer in the guanine-cytosine base pair and suggested that in ionized and excited

* A preliminary account has been presented at the First International Congress of Quantum Chemistry, Menton, France, 1973, and has appeared in Ref. [3].

** Present address: Institute of Physical and Chemical Research, Wako, Saitama 351, Japan.

states the proton is more easily transferred from guanine to cytosine than in the ground state. Clementi, Mehl, and von Niessen [10] performed very accurate SCF calculations of the guanine-cytosine pair and the formic acid dimer for the ground state only. They found that the transfer of a single proton from one molecule to another gave a potential curve which was monotonically increasing as the proton was transferred. Only when two bridging protons were simultaneously and symmetrically moved, the potential energy curve with a double minimum was obtained. One of the purposes of the present study is to calculate the potential energy curves for excited states with *ab initio* methods.

Another interesting aspect is related to the resonance interaction in the excited state. The formic acid dimer consists of two identical molecules and an excited state of the monomer is split to two states in the dimer. This splitting, under some conditions, is observable in the electronic spectroscopy [11], and is related to the dynamic behavior, such as the lifetime, of the excited state.

2. Method

2.1. Geometry and Basis Sets

The geometry of the formic acid dimer was taken from Clementi *et al.* [10], which was based on the electron diffraction experiment [12] and shown in Fig. 1. Two hydrogen-bonded protons, H_2 and H_4, are moved along the O_2-O_3 and O_1-O_4 axes, respectively, maintaining the overall C_{2h} symmetry, while keeping the other geometry parameters at the experimental values. Calculations were performed for six geometries with a fixed O_2-O_3 and O_1-O_4 distance (2.730 Å); *I* ($R_{O_2H_2} = R_{O_4H_4} = 0.874$ Å, $R_{H_2O_3} = R_{H_4O_1} =$ 1.856 Å), *II* (0.980, 1.750) which is experimental geometry, *III* (1.192, 1.538), *IV* (1.404, 1.326), *V* (1.616, 1.114), and *VI* (1.828, 0.902). We also use this designation to describe the geometry of a monomer as a function of $R_{O_2H_2}$. In order to compare the potential energy curve for the dimer with that for the monomer, calculations for the monomer with a stretched O-H bond were also carried out. The analytical expression for the potential energy curve is obtained by fitting the calculated energies to a polynomial.

The basis set used is the STO-3G *p* set, i.e., the STO-3G set with standard exponents and scale factors [13], augmented with a diffuse *p*-type orbital on carbon and oxygen atom with an exponent 0.06 and 0.106, respectively. The extensive studies on the basis set dependency (including this set) of the hydrogen-bonding energy have been reported in previous papers of the present series [4, 5].

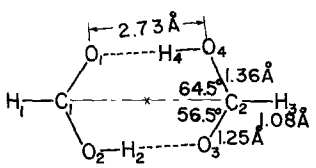

Fig. 1. The geometry of the dimer. Refs. [10] and [12]

2.2. Two-Configuration Electron-Hole Potential (TCEHP) Method

In the previous papers we employed the electron-hole potential (EHP) method [7] to study excited states of hydrogen-bonding complexes [4, 5] and electron donor-acceptor complexes [14]. In the EHP method the wave function of excited state is described by a single electron configuration with a correct spin symmetry:

$$\Psi(\alpha \to \mu) = \frac{1}{\sqrt{2}} (a^{\dagger}_{\mu\uparrow} a_{\alpha\uparrow} \pm a^{\dagger}_{\mu\downarrow} a_{\alpha\downarrow}) \Phi^0 \tag{1}$$

where + and – signs stand for the singlet and triplet states, respectively, and $a_{\alpha\uparrow}$ and $a^{\dagger}_{\mu\uparrow}$ are annihilation and creation operators for the one-particle functions ϕ_α and ϕ_μ with an alpha spin while $\downarrow$ refers to a beta spin. Φ^0 is the SCF wave function for the closed shell ground state. The one-particle functions, ϕ_α and ϕ_μ, which are interpreted as the orbitals for a hole and an electron, are determined within the occupied orbital space and within the vacant orbital space, respectively, of the SCF ground state in such a way that the energy $E(\alpha \to \mu) = \langle \Psi(\alpha \to \mu) | H | \Psi(\alpha \to \mu) \rangle$ is minimized [7]. Consequently, the functions ϕ_α and ϕ_μ are different from the canonical SCF orbitals. The wave function (1) has been shown to be a good variational approximation to the wave function of the full single-excitation configuration mixing calculation (the so-called Tamm-Duncoff approximation) [4, 5].

The one-configuration description, however, cannot be used for excited states of a dimer, M_1M_2, composed of the identical molecules, M_1 and M_2, because here one has to take into account the resonance interaction [11, 15] between two states $M_1M_2^*$ and $M_1^*M_2$, where M_i^* denotes an excited state of a monomer M_i. For example, suppose an excited state of a monomer, M_1^*, can be described by a wave function,

$$\Psi_{M_1}(\alpha_1 \to \mu_1) = \frac{1}{\sqrt{2}} (a^{\dagger}_{\mu_1\uparrow} a_{\alpha_1\uparrow} \pm a^{\dagger}_{\mu_1\downarrow} a_{\alpha_1\downarrow}) \Phi^0_{M_1} \tag{2}$$

where $\Phi^0_{M_1}$ is the ground state SCF wave function of M_1. When the distance between M_1 and M_2 is large enough, the ground state wave function of the dimer can be given as

$$\Psi^0_{M_1M_2} = \mathscr{A} \Phi^0_{M_2} \Phi^0_{M_1} \tag{3}$$

where $\mathscr{A}$ is an antisymmetrizer. Two excited states $\Psi^0_{M_1M_2}(\alpha_1 \to \mu_1)$ and $\Psi^0_{M_1M_2}(\alpha_2 \to \mu_2)$:

$$\Psi^0_{M_1M_2}(\alpha_i \to \mu_i) = \frac{1}{\sqrt{2}} (a^{\dagger}_{\mu i\uparrow} a_{\alpha i\uparrow} \pm a^{\dagger}_{\mu i\downarrow} a_{\alpha i\downarrow}) \Psi^0_{M_1M_2}, \qquad i = 1 \text{ and } 2 \tag{4}$$

are degenerate. This degeneracy is lifted by the resonance interaction:

$$\langle \Psi^0_{M_1M_2}(\alpha_1 \to \mu_1) | H | \Psi^0_{M_1M_2}(\alpha_2 \to \mu_2) \rangle.$$

Therefore, a linear combination of the two configurations is required for the correct description of excited states of the dimer. The correct forms of the wave function are

$$\Psi^{\pm}_{M_1M_2}(\alpha \to \mu) = \frac{1}{\sqrt{2}} (\Psi^0_{M_1M_2}(\alpha_1 \to \mu_1) \pm \Psi^0_{M_1M_2}(\alpha_2 \to \mu_2)) \tag{5}$$

for the dimer with an inversion or a plane of symmetry. In (5) ± corresponds to gerade and ungerade, or symmetric and antisymmetric, respectively. The wave function (5) can be rewritten as

$$\Psi^{\pm}_{M_1M_2}(\alpha \to \mu) = \frac{1}{2\sqrt{2}} [\{(a^{\dagger}_{\mu_1\uparrow} + a^{\dagger}_{\mu_2\uparrow})(a_{\alpha_1\uparrow} \pm a_{\alpha_2\uparrow}) + (a^{\dagger}_{\mu_1\uparrow} - a^{\dagger}_{\mu_2\uparrow})(a_{\alpha_1\uparrow} \mp a_{\alpha_1\uparrow})\} + \{(a^{\dagger}_{\mu_1\downarrow} + a^{\dagger}_{\mu_2\downarrow})(a_{\alpha_1\downarrow} \pm a_{\alpha_2\downarrow}) + (a^{\dagger}_{\mu_1\downarrow} - a^{\dagger}_{\mu_2\downarrow})(a_{\alpha_1\downarrow} \mp a_{\alpha_2\downarrow})\}] \Phi^0_{M_1M_2} \tag{6}$$

for the singlet state. The operators $(1/\sqrt{2})(a^{\dagger}_{\mu_1} \pm a^{\dagger}_{\mu_2})$ and $(1/\sqrt{2})(a_{\alpha_1} \pm a_{\alpha_2})$ are the operators for the super-molecular orbitals $\phi^{\pm}_{\mu} = (1/\sqrt{2})(\phi_{\mu_1} \pm \phi_{\mu_2})$ and $\phi^{\pm}_{\alpha} = (1/\sqrt{2}) \times (\phi_{\alpha_1} \pm \phi_{\alpha_2})$ which are delocalized over two molecules, M_1 and M_2. Therefore, a linear combination of at least two electron configurations, the excitations $\phi^{+}_{\alpha} \to \phi^{+}_{\mu}$ and $\phi^{-}_{\alpha} \to \phi^{-}_{\mu}$, or $\phi^{-}_{\alpha} \to \phi^{+}_{\mu}$ and $\phi^{+}_{\alpha} \to \phi^{-}_{\mu}$ is required to lift the near-degeneracy between two excitations that are completely degenerate at the infinite separation.

Thus, in order to apply the EHP method to studying an excited state of a dimer of two identical molecules, the EHP method must be extended to the two-configuration wave function [8]. We assume that the wave function of an excited state can be written as a linear combination of two electron configurations:

$$\Psi_{TC} = B_{\alpha\mu}\Psi(\alpha \to \mu) + B_{\beta\nu}\Psi(\beta \to \nu). \tag{7}$$

In the two-configuration EHP (TCEHP) method, the CI coefficients, $B_{\alpha\mu}$ and $B_{\beta\nu}$, as well as ϕ_{α}, ϕ_{β}, ϕ_{μ} and ϕ_{ν}, are variationally determined. The TCEHP method is the simplest version of the multi-configuration self-consistent field (MCSCF) method. The equations to be solved, the procedure to solve them, and properties of the TCEHP wave function are presented in separate papers [8, 16] [1]. As in the one-configuration electron-hole potential method, the orbitals ϕ_{α} and ϕ_{β} are determined within the occupied orbital space of the SCF ground state, while the orbitals ϕ_{μ} and ϕ_{ν} are optimized within the vacant orbital space. The wave function (7) satisfies the generalized Brillouin theorem: the off-diagonal elements of Hamiltonian matrix between (7) and such excitations as $\Psi(\alpha \to \eta)$, $\Psi(\beta \to \eta)$, $\Psi(\gamma \to \mu)$ and $\Psi(\gamma \to \nu)$ vanish, where ϕ_{γ} and ϕ_{η} are the orbitals determined within the occupied and vacant orbital spaces, respectively, and are orthogonal to ϕ_{α}, ϕ_{β}, ϕ_{μ} and ϕ_{ν} [8].

2.3. Decomposition of the Dimerization Energy

In order to elucidate the origin of hydrogen-bonding interaction it is often very instructive to analyze individual components of interaction energy. Morokuma developed a scheme within the Hartree-Fock method of total interaction energy of the ground state into the electrostatic, exchange-repulsion, polarization, and charge-transfer (electron-delocalization) energies [1a]. Iwata and Morokuma extended the scheme

[1] Actually coded equations are Eq. (18) in Ref. [8] with the assumption $\delta\lambda_{\alpha\alpha}$, $\delta\lambda_{\beta\beta}$, $\delta\lambda_{\alpha\beta}$ and $\delta\lambda_{\beta\alpha} = 0$. Eq. (21) in Ref. [8] does not work. An alternative and better way to solve the coupled equation for TCEHP will be presented in a separate paper [16].

into a form applicable to the analysis of the interaction energy in the excited state, whose wave function is given by the EHP method. In the present paper the scheme is further extended for the interaction energy in the excited state described by the TCEHP method.

Since the O-H distance in a formic acid dimer is different from that of a monomer in the present calculations, the dimerization energy $\Delta E(R, r)$ must be defined for the dimer with the intermolecular distance, R, and the O_2-H_2 (and O_4-H_4) bond distance, r, as

$$\Delta E(R, r) = E_4(R, r) - E(\infty, r_e) \tag{8}$$

where E_4 is the energy of the SCF or TCEHP calculation for the dimer and r_e is the equilibrium O-H distance for the monomer. The dimerization energy can be further decomposed into components [1a, 4a]:

$$\begin{aligned} \Delta E(R, r) &= \{E_4(R, r) - E_3(R, r)\} && \text{charge-transfer plus polarization} \\ &+ \{E_3(R, r) - E_1(R, r)\} && \text{exchange repulsion} \\ &+ \{E_1(R, r) - E(\infty, r)\} && \text{electrostatic} \\ &+ \{E(\infty, r) - E(\infty, r_e)\} && \text{O-H bond weakening} \\ &\equiv E_{\mathrm{ct+pl}} + E_{\mathrm{ex}} + E_{\mathrm{es}} + E_{\mathrm{bw}} \end{aligned} \tag{9}$$

where $E_1(R, r)$ and $E_3(R, r)$, as defined in Ref. [1a], are evaluated with and without the zero differential overlap approximation between two molecules, respectively, by using the wave function (6) in which all molecular orbitals are determined for an isolated monomer with the O-H bond distance r. $E_1(R, r) - E(\infty, r)$ is the electrostatic energy E_{es}, and $E_3(R, r) - E_1(R, r)$ is the exchange repulsion energy E_{ex}. The separation of E_{ct} and E_{pl} is not carried out in the present paper [17][2]; The magnitude of the interaction in the excited state can be directly evaluated from the splitting of the ± states.

The actual procedure for evaluating E_1 is simple even in the TCEHP method, because all the orbitals are orthonormal because of the zero-differential overlap approximation. The procedure for E_3 is rather cumbersome in the TCEHP method and is given in the appendix in detail.

3. Results and Discussion

3.1. Molecular Symmetry

The molecular point groups of the formic acid monomer and dimer are C_s and C_{2h}, respectively. The correlation of the molecular orbitals and states of the monomer and the dimer is given in Table 1.

---

[2] E_{ct} in this present scheme includes the true charge transfer energy E_{CT} and a coupling term E_{MIX}. See Ref. [17].

Table 1. Correlation diagram for the molecular symmetry

	Monomer	Dimer
Point Group	C_s	C_{2h}
n and σ Orbitals	a'	$\begin{cases} -^a & b_u \\ +^a & a_g \end{cases}$
π Orbitals	a''	$\begin{cases} -^a & b_g \\ +^a & a_u \end{cases}$
$n \rightarrow \pi^*$ and $\sigma \rightarrow \pi^*$ States	A''	$\begin{cases} & A_u \\ & B_g \end{cases}$
$\pi \rightarrow \pi^*$ and $\sigma \rightarrow \sigma^*$ States	A'	$\begin{cases} & A_g \\ & B_u \end{cases}$

[a] Sign of the linear combination of two monomer orbitals.

3.2. *Orbital Energies and Ionization Potentials*

The geometry parameters in the monomer calculations, except for the O_2-H_2 distance, are fixed in the same manner as the dimer. The calculated equilibrium O_2-H_2 distance for the monomer is 1.00 Å (experimentally 0.95 Å) and is indistinguishable with that of the dimer within the accuracy of our search. The electron configuration of the SCF ground state of the monomer is

$$(1a')^2\ (2a')^2\ (3a')^2\ (4a')^2\ (5a')^2\ (6a')^2\ (7a')^2\ (8a')^2\ (1a'')^2\ (9a')^2\ (2a'')^2\ (10a')^2,$$

where the orbitals are in order of their canonical orbital energies. In Fig. 2, the change of the orbital energies for the monomer and the dimer as functions of $R_{O_2H_2}$ is shown. In Fig. 2, and hereafter, both M and M′ denote the monomer; M being the regular monomer and M′ being a monomer with H bonded to O_1, rather than O_2 where $R_{CO_2} > R_{CO_1}$. Calculations for the monomer M′ were carried out for comparison with the dimers having a longer $R_{O_2H_2}$ (the geometries *V* and *VI*).

The $10a'$ orbital is the non-bonding (lone-pair) orbital of the carbonyl oxygen, while the $2a''$ is a π orbital mainly localized on the oxygen atom of the hydroxy group. The energies of both orbitals increase only slightly with the weakening of the O_1-H bond and split by a small amount upon dimer formation. The orbital ordering of $10a'$ and $2a''$ is reversed in M′. The third highest occupied orbital, $9a'$, and the second lowest vacant orbital, $11a'$, of monomer are the bonding and anti-bonding orbitals of the O-H bond, respectively. Consequently, the orbital energy of $9a'$ increases, and that of $11a'$ decreases with the O_2H bond distance. The splitting of the $9a'$ orbital upon the dimer formation is large, and the orbital energy of one of the components ($9b_u$) reaches as high as that of $9a'$ of the monomer.

The ionization potentials of the monomer and the dimer calculated by Koopmans' theorem are given in Table 2 with the observed vertical ionization potentials [18, 19]. The geometry used for the dimer and the monomer is *II*, the experimental one. As is known, Koopmans' theorem overestimates the ionization potential; if a scale factor, 0.92, is

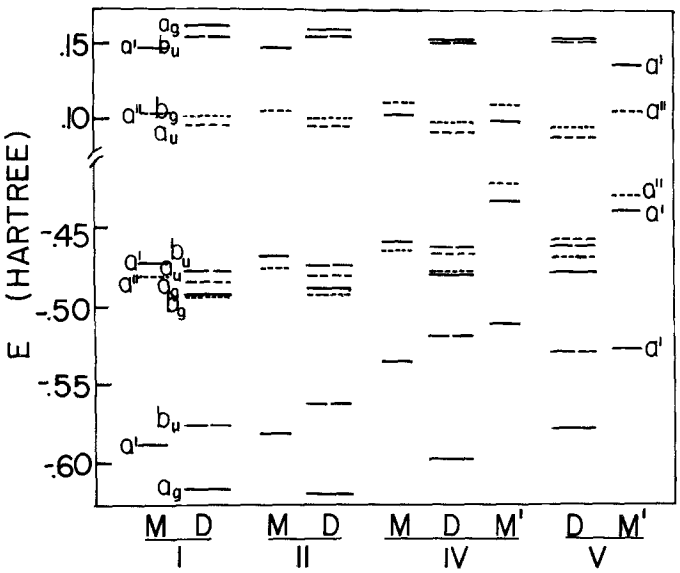

Fig. 2. The orbital energy diagram. The D, M, and M' stand for the dimer, the monomer with an O_2H bond, and the monomer with an O_1H bond. The O_2H_2 bond distance for the geometries *I, II, . . .*, and *VI* is given in text

Table 2. Vertical ionization potentials (eV)

Monomer				Dimer			
Orbital	Koopmans'	(x 0.92)	Obsd.[a,b]	Orbital	Koopmans'	(x 0.92)	Obsd.[b]
$10a'(n)$	12.8	(11.8)	11.5	$10b_u(n)$	13.0	(12.0)	11.3
$2a''(\pi)$	13.0	(12.0)	12.5	$2a_u(\pi)$	13.1	(12.1)	11.7
				$10a_u(n)$	13.4	(12.3)	∫
				$2b_g(\pi)$	13.4	(12.3)	12.5
$9a'(\sigma_{OH})$	15.9	(14.6)	14.8	$9b_u(\sigma_{OH})$	15.4	(14.2)	14.1

[a] Ref. [18]. [b] Ref. [19].

multiplied to Koopmans' ionization potential, as is often done [20], a closer agreement between theoretical and observed vertical ionization potentials is obtained (see in the parentheses in Table 2). In the UV excitation photoelectron spectra of the dimer [19], two bands at 11.3 and 14.1 eV, and a broad band between 11.7 and 12.5 eV have been observed. The first and the broad bands may be assigned to the ionizations of the non-binding and π orbitals ($10b_u$, $2a_u$, $10a_g$, and $2b_g$). These ionization potentials are shifted, experimentally, slightly to the lower energy upon dimer formation, while, theoretically, slightly to the higher side. If we assign the third band at 14.1 eV to the ionization of the $9b_u$ orbital, the dimerization shift of this band is toward lower energy in accord with the theory.

3.3. Vertical Excitation Energies

The vertical excitation energies of the monomer are calculated at the geometry *II* by using the one-configuration (OCEHP) and two-configuration (TCEHP) electron-hole potential methods. The results are given in Table 3, compared with the energies obtained by the calculations based on the canonical SCF orbitals. In the TCEHP calculations, the linear combinations,

$$C_1(10a' \rightarrow 3a'') + C_2(2a'' \rightarrow 11a'), \qquad \text{for the } A''(n\text{-}\pi^*) \text{ excited state,} \tag{10a}$$

$$C_3(2a'' \rightarrow 3a'') + C_4(10a' \rightarrow 11a'), \qquad \text{for the } A'(\pi\text{-}\pi^*) \text{ excited state} \tag{10b}$$

are taken as the starting wave functions. The first configuration of the above combinations is used for OCEHP. In other words, the TCEHP wave functions for the monomer contain the effects of the interaction between the excitations $(n(\sigma) \rightarrow \pi^*)$ and $(\pi \rightarrow \sigma^*)$ for the A'' excited state and between the excitations $(\pi\text{-}\pi^*)$ and $(n(\sigma) \rightarrow \sigma^*)$ for the A' excited state. As is seen in Table 3, the large energy stabilization over the canonical orbital method is obtained for the $^3A''(n\text{-}\pi^*)$, $^1A''(n\text{-}\pi^*)$, and $^3A'(\pi\text{-}\pi^*)$ by the OCEHP method. Therefore, one can say that in these three states the effect of the second electron configuration (angular correlation) is very small and negligible. In the previous paper [8], we have shown that if the energy of OCEHP is in good agreement with that of TCEHP, the energy of both EHP is in good approximation to that of the Tamm-Duncoff approximation or the CI of all singly excited configurations. The above fact indicates that the OCEHP method is a good approximation for the lowest $^1A'$, $^3A''$ and $^3A'$ states of the monomer. This means that two configurations, one for the excitation of each monomer, is sufficient to describe the corresponding state of the dimer, and therefore we use the TCEHP method for dimer calculation.

The advantage of the EHP methods could be seen if the number of configurations which have to be included in the Tamm-Duncoff approximation is counted. With the present basis set, these are 60 and 108 configurations for A'' and A' states of the monomer, and 120, 120, 216, and 216 for A_u, B_g, A_g and B_u of the dimer, respectively, while TCEHP requires only two configurations for each symmetry.

The calculated vertical transition energy to the $^1A''(n\text{-}\pi^*)$ state is in good agreement with experiments [21]. The EHP method in general gives reasonably good results for the transition energies to the $(n\text{-}\pi^*)$ states [4, 5, 8]. It is not known experimentally

Table 3. The vertical excitation energies of formic acid monomer (eV)

	Canonical Orbitals		Electron Hole Potential		
	One Conf.	Two Conf.	One Conf.	Two Conf.	Experiments
$^3A''$ $^3(n\text{-}\pi^*)$	7.58	7.58	5.13	5.12	
$^1A''$ $^1(n\text{-}\pi^*)$	7.94	7.94	5.83	5.83	>5.8[a]
$^3A'$ $^3(\pi\text{-}\pi^*)$	7.79	7.79	4.91	4.85	
$^1A'$ $^1(\pi\text{-}\pi^*)$	11.13	10.75	11.01	9.84	~8.4[a]

[a] Ref. [21].

which of the $^3A''(n\text{-}\pi^*)$ and $^3A'(\pi\text{-}\pi^*)$ is the lowest triplet state. The relative order of the triplet $(n\text{-}\pi^*)$ and $(\pi\text{-}\pi^*)$ states is sensitive to the environment of the carbonyl group. In the theoretical calculation it also depends on the size and type of basis set used [5, 6], and therefore no definite conclusion on the relative order can be drawn from the present calculation.

For the $^1A'(\pi\text{-}\pi^*)$ state the second electron configuration in the TCEHP wave function gives the substantial effect on the energy, as is seen in the last row of Table 3. The TCEHP procedure, however, still gives a calculated vertical excitation energy much higher than observed. This fact might be related to the well-known difficulties found in studies of the $\pi\text{-}\pi^*$ singlet states of many molecules [22–24], but will not be pursued here.

As is mentioned in Sect. 2.2, it is necessary to use the TCEHP method for the description of excited states of a dimer, even when the OCEHP wave function is reasonably reliable for the corresponding excited states of monomer, as in the present reliable case [25][3]. Thus the linear combinations

$$\begin{aligned}
&C_1(10b_u \rightarrow 3a_u) + C_2(10a_g \rightarrow 3b_g) && \text{for the } B_g(n\text{-}\pi^*) \text{ state}\\
&C_3(10a_g \rightarrow 3a_u) + C_4(10b_u \rightarrow 3b_g) && \text{for the } A_u(n\text{-}\pi^*) \text{ state}\\
&C_5(2a_u \rightarrow 3a_u) + C_6(2b_g \rightarrow 3b_g) && \text{for the } A_g(\pi\text{-}\pi) \text{ state}\\
&C_7(2b_g \rightarrow 3a_u) + C_8(2a_u \rightarrow 3b_g) && \text{for the } B_u(\pi\text{-}\pi^*) \text{ state}
\end{aligned} \qquad (11)$$

are used in the TCEHP calculations of the dimer. In these approximations the energies of the dimer must be compared with the OCEHP results of the monomer. The vertical excitation energies of the dimer at the experimental geometry, *II*, are given in Fig. 3,

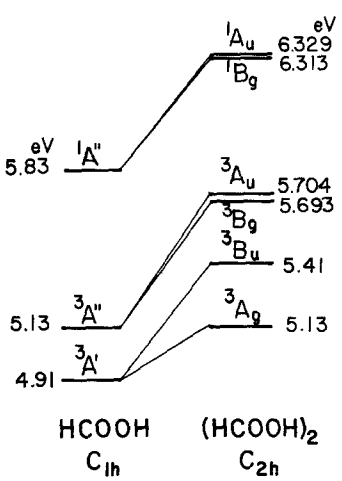

Fig. 3. OCEHP excitation energies of the formic acid monomer, and TCEHP excitation energies of the dimer at the experimental geometry *II*

[3] A similar situation was found in studies of the excited states of glyoxal (HCOCHO). The proper description of the excited states of dicarbonyls such as glyoxal requires a linear combination of at least two electron configurations [25].

along with the corresponding energies of the monomer. All of the transition energies calculated increase with the dimer formation. The splittings between B_u and A_g states and between A_u and B_g states are caused by the resonance interaction between the corresponding excited states of the monomers. The splitting of the singlet and triplet n-π^*(A_u and B_g) states is very small (0.017 and 0.011 eV, respectively). The splitting in the ^3B_a and ^3A_g states is relatively large (0.275 eV). In all three pairs of excited states, the gerade (g) state has a lower energy than the corresponding ungerade (u) state. Since the transition from the ground state is allowed only to a u state, the photo-excitation always brings the dimer to the upper state of the pair, from which subsequently it falls to the lower state. This lower state would have a long lifetime because the transition from it to the ground state is forbidden [11].

3.4. Potential Energy Curves for the Symmetrical Proton Exchange

First, in order to demonstrate that the present small basis set calculations can produce a reasonable potential energy curve for the symmetrical proton exchange in the ground state of the formic acid dimer, earlier results calculated with large basis sets by Clementi *et al.* [10] are compared with ours in Fig. 4 and Table 4. Since the difference of the total electron energies is large, the curves are shifted in such a way that the points at the experimental geometry (*II*) coincide with each other. The agreement is extremely good.

The potential curves are given in Figs. 5-8 for the ground, $^3(\pi$-$\pi^*)$, $^3(n$-$\pi^*)$, and $^1(n$-$\pi^*)$ states of the monomers and the dimer. As is mentioned in Sect. 3.3, there are two states in the dimer, which correspond to one state in the monomer. In each figure we show only the lower state of the two, namely, ^3A_g, ^3B_g, and ^1B_g in Figs. 6, 7, and 8, respectively. The curve for the higher (ungerade) state is almost parallel with that of the lower. In order to compare curves between monomers and dimers, they are shifted so that the minimum points of the monomer coincide with that of the dimer. The calculated equilibrium $R_{O\text{-}H}$ distance in all states studied of the monomer and the dimer is approximately 1.00 Å.

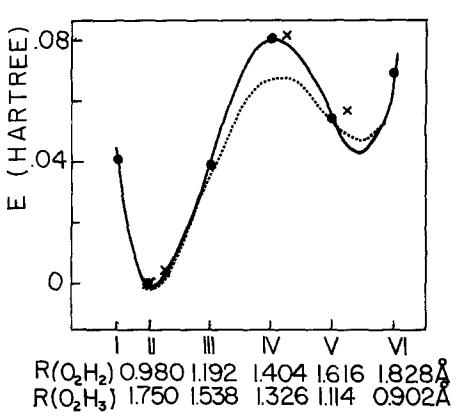

Fig. 4. The ground state potential energy curve as functions of $R_{O_2H_2}$ for three basis sets. —•—: The present results (3G + p); -----: (9/5) results by Clementi *et al.* [10]; X: (9/5 + polarization functions) results by Clementi *et al.* [10]. The ordinate is relative to the energies at the experimental geometry (which are −372.88571, −377.14839, and −377.31018 Hartree for (3G + p), (9/5), and (9/5 + pol.), respectively

Table 4. Positions (Å) of maximum and minima and barrier heights (kcal/mole) for the symmetric proton exchange in the formic acid dimer

Basis Set	9/5[a]	STO-3G + p			
State	Ground	Ground	^3A_g (π-π^*)	^3B_g (n-π^*)	^1B_g (n-π^*)
First Minimum: $R_{O_2H_2}$	0.99	1.00	0.99	1.00	1.00
$V_1 = E$(Max) − E(1st Min)	43.0	51.0	66.2	76.8	73.6
Maximum: $R_{O_2H_2}$	1.44	1.42	1.40	1.43	1.42
$V_2 = E$(Max) − E(2nd Min)	13.5	23.6	41.5	55.9	54.6
Second Minimum: $R_{O_2H_2}$	1.72	1.72	1.76	1.75	1.75
$R_{O_3H_2}$	1.01	1.01	0.97	0.98	0.98
$V_1 - V_2$	29.5	27.4	24.7	2.09	19.0

[a] Ref. [10].

The shapes of the potential curves for the monomer M are similar for all states; in fact, the lowest vibrational states of the O-H stretching are $E(v = 0) = 1970$ cm^{-1} and $E(v = 1) = 5850$ cm^{-1} in all states. This result is partly due to the assumed geometry parameters other than R_{OH}. If the other parameters such as C=O_1, and C-O_2 distances are also optimized for each state, the equilibrium R_{OH} distance is expected to change. But this is also partly due to the nature of the excited states in which only n and π electrons not directly contributing to the OH bond are excited.

The energy of the monomer M′, where a hydrogen atom is attached to the oxygen O_1 which has a shorter CO_1 bond, is much higher than that of the normal monomer for the ground, and the n-π^* singlet and triplet states. For the $^3A'\pi$-π^* state, however, both monomers, M and M′, with equal R_{O_2H} and R_{O_1H}, respectively, have almost

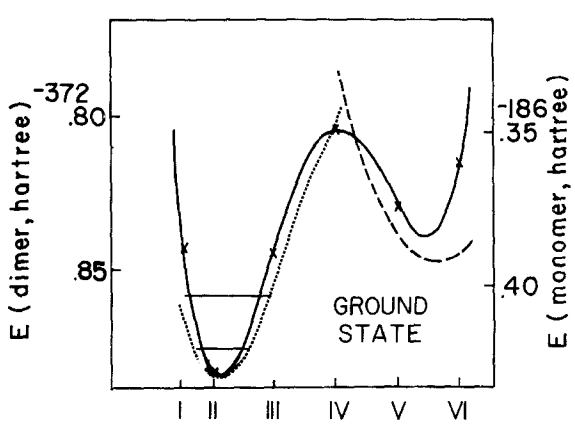

Fig. 5. The potential curve (——) of the ground state dimer as a function of $R_{O_2H_2} = R_{O_4H_4}$, and the curves of the ground state monomer M (- - - -) as a function of R_{O_2H} and of the monomer M′ (— —) as a function of R_{O_1H}. The horizontal lines indicate the two lowest vibrational states of the monomer

equal energy. This is understandable since the π-π^* excitation of the formic acid monomer is an intramolecular charge-transfer from O_2 to O_1:

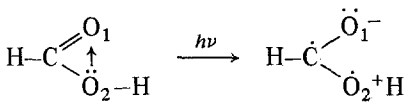

(12)

In all the geometries studied, the lowest triplet $^3A'$ state remains to be essentially a π-π^* excitation. On the other hand, the lowest singlet $^1A'$ state changes its characteristics drastically with the R_{O_2H} distance: the main electron configuration in Eq. (10b) changes around R_{O_2H} = 1.3 Å from the first configuration (π-π^*) to the second (n or $\sigma \rightarrow \sigma^*$). Because of this strong interaction between configurations, at least four configurations must be considered for description of the π-π^* singlet excited states of the dimer.

The characteristics of the potential curves of the dimer are summarized in Table 4, where the numbers are evaluated by a polynomial fit of the calculated energies. As has been mentioned, features of our potential curve for the ground state are generally in agreement with that of the 9/5 results of Clementi *et al.* [10], though the barrier heights of the present calculations are slightly higher. The positions of the maximum and minima are found to be almost independent of states. The barrier heights in all three excited states studied are higher than that of the ground state. The potential curves of the triplet and singlet $B_g(n\text{-}\pi^*)$ states are very similar to each other. We have noticed in other studies of hydrogen bonding in excited states [4–6] a triplet and singlet n-π^* state always has similar characteristics, which is in contrast to the case of triplet and singlet π-π^* excited states. Since the potential curve for the singlet $^1A'$ state of the formic acid monomer differs from that for the triplet $^3A'$ state, it is expected that the potential curves of $^1A_g(\pi\text{-}\pi^*)$ and $^1B_u(\pi\text{-}\pi^*)$ states are different from those of the corresponding triplet states.

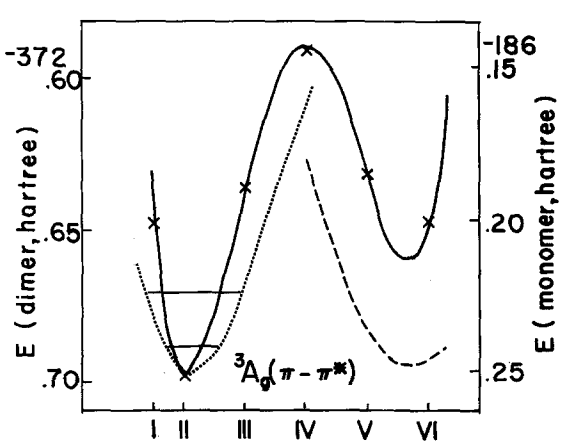

Fig. 6. The potential curves of the $^3A_g(\pi\text{-}\pi^*)$ dimer and the $^3A'$ monomers. See Fig. 5 for details

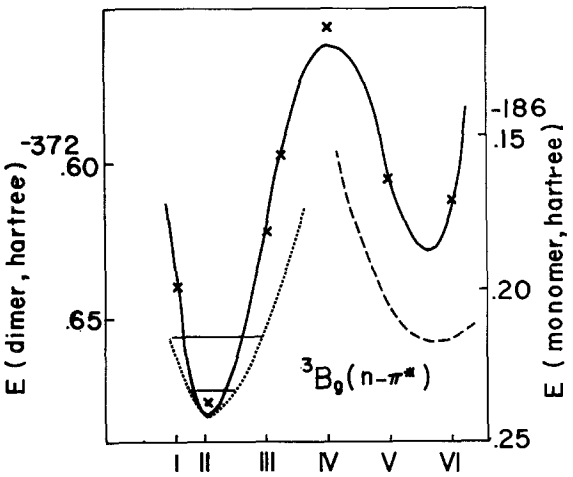

Fig. 7. The potential curves of the $^3B_g(n\text{-}\pi^*)$ dimer and the $^3A''$ monomers. See Fig. 5 for details

3.5. Hydrogen-Bonding Energy and its Components

The calculated hydrogen-bonding energy of the formic acid dimer is given in Table 5 along with that of formaldehyde-water and acrolein-water complexes. Shifts of the vertical excitations caused by the complex formation are also shown in the Table 5. The hydrogen-bonding energy of the formic acid dimer, even divided by 2, is the largest of three systems, which is due to the shorter $O_1 \ldots H_4$ distance (1.75 Å experimentally) in the formic acid dimer than in the formaldehyde-water (1.89 Å calculated [1a]). Even in the n-π^* excited states relatively large hydrogen-bonding energies are obtained in the formic acid dimer, which is a marked difference from the other hydrogen-bonding systems. That is to say, the present calculations show that the n-π^* excited states (excimer states) of the formic acid dimer is stable for dissociation, while the n-π^* excited states (exciplex states) of the formaldehyde-water and acrolein-water complexes are rather dissociative. Though the excited states of the formic acid dimer are stable, large blue shifts of the vertical transitions are expected because the ground state dimer is much more stable.

Table 5. Calculated hydrogen-bond energies (kcal/mole)[a] and shifts of the vertical transition energies in parentheses (cm^{-1})

Complexes	$(HCOOH)_2$	H_2CO-HOH[b]		$H_2CHCHCO$-HOH[c]	
Basis set	3G + p	3G + p	3G	3G + p	3G
Ground	−17.5	−5.6	−3.4	−7.4	−4.1
$^3(\pi\text{-}\pi^*)$	−12.3 (+1820)	−1.4 (+1450)	−2.1 (+440)	−7.7 (−100)	−4.3 (−60)
$^3(n\text{-}\pi^*)$	− 4.4 (+4570)	+0.6 (+2180)	+1.0 (+1530)	+0.6 (+2780)	+1.4 (+1940)
$^1(n\text{-}\pi^*)$	− 6.3 (+3920)	−0.1 (+1940)	−0.1 (+1160)	−0.5 (+2420)	+0.2 (+1490)

[a] A negative value corresponds to stabilization, while positive to destabilization.
[b] Ref. [4].
[c] Ref. [5].

Table 6. Hydrogen bonding energy and its components[a] (kcal/mole)

Geometry	State	Components				
		ΔE	E_{bw}	E_{es}	E_{ex}	E_{ct+pl}
I	Ground	8.2	24.2	−25.6	22.6	−13.1
	$^3(\pi\text{-}\pi^*)$	17.4	23.9	−19.9	22.4	− 9.0
	$^3(n\text{-}\pi^*)$	18.6	23.8	−11.6	18.9	−12.5
	$^1(n\text{-}\pi^*)$	17.2	24.0	−11.7	19.1	−14.1
II	Ground	−17.5	0.0	−31.4	31.9	−17.9
	$^3(\pi\text{-}\pi^*)$	−12.3	0.0	−25.1	31.8	−19.0
	$^3(n\text{-}\pi^*)$	− 4.4	0.0	−15.5	27.6	−16.5
	$^1(n\text{-}\pi^*)$	− 6.3	0.0	−15.6	27.7	−18.4
III	Ground	7.2	37.3	−49.7	62.3	−42.6
	$^3(\pi\text{-}\pi^*)$	25.7	37.8	−41.6	63.0	−33.6
	$^3(n\text{-}\pi^*)$	29.8	38.0	−27.8	56.7	−37.1
	$^1(n\text{-}\pi^*)$	26.3	37.7	−27.9	56.9	−40.3

In Table 6, the results of the energy decomposition analysis based on Eq. (9) are given in the geometries *I*, *II* and *III*. It is clear that both E_{es} and E_{ct+pl} are responsible for the large hydrogen-bonding energy, ΔE, in all states. The principal difference between states is due to the difference in E_{es}. E_{ct+pl} is rather independent of states, as was seen in other hydrogen-bonding systems studied previously [4, 5].

A comparison of energy components between different hydrogen-bonding systems is also interesting. For the equilibrium geometry of the ground state of $H_2CO \cdots HOH$ [4] and $H_2C{=}CH{-}CHO \cdots HOH$ [5], the energy components ($\Delta E, E_{es}, E_{ex}, E_{pl+ct}$) are (−5.6, −11.4, +10.9, −5.1 kcal/mole) and (−7.4, −13.1, +11.6, −5.9), respectively, with the same basis set as in the present paper. The formic acid dimer, which has a much smaller O ··· O distance (2.73 Å) than these complexes (2.89 Å, calculated [4]), yields very different energy components: (−8.8, −15.7, +16.0, −9.0)

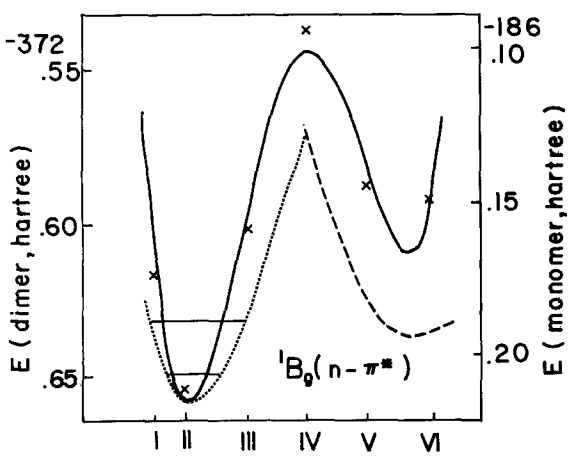

Fig. 8. The potential curves of the $^1B_g(n\text{-}\pi^*)$ dimer and the $^1A''$ monomers. See Fig. 5 for details

per hydrogen bond. The magnitude of all the energy components of $(HCOOH)_2$ is larger than that of the others. The relative importance of E_{ct+pl} is more profound in $(HCOOH)_2$.

4. Concluding Remarks

In the present study we could not find a state with a low barrier for the hydrogen exchange through the hydrogen-bond bridge. This might be partly due to the lack of geometry optimization for excited states. However, the nature of excitation suggests that the high barrier is a true characteristic of the lower excited states we studied. The orbitals involved in that excitations studied are the lone pair (n) orbital of the hydroxy oxygen and π and π^* orbitals mainly localized in the carbonyl group. Since these orbitals are not directly involved in the weakening of the O_2-H_2 bond or the strengthening of the $H_2 \cdots O_3$ bond, the barrier is not expected to change drastically upon these excitations. States which may have a substantial low barrier of proton exchange are those which involve an excitation from the O_2-H_2 σ orbital or to the O_2-H_2 σ^* orbital. Some states might even have a symmetric hydrogen bond, i.e., a single potential minimum with the hydrogen atom situated near the midpoint between two oxygen atoms. In this connection the $^1A'(\pi \rightarrow \pi^*)$ state of formic acid is an interesting state. As was discussed in Sect. 3.4, as one stretches the O_2-H_2 distance, an n or $\sigma \rightarrow \sigma^*$ configuration becomes extremely important. Therefore, through this mixing the lowest ^1A_g or $^1B_u(\pi \rightarrow \pi^*)$ states may actually have a barrier lower than the states we have studied. For a calculation of such states, an MCSCF calculation with four or more configurations or an extensive CI calculation would be required.

Acknowledgement. The authors are grateful to Dr. W. A. Lathan for helpful discussions. The research has been supported in part by the National Science Foundation and the Center for Naval Analyses of the University of Rochester.

Appendix. Evaluation of E_3 for an Excited State Described by a TCEHP Wave Function

E_3 in the energy decomposition analysis is the energy associated with the wave function

$$\Psi_3 = \mathscr{A}\Psi_A\Psi_B \tag{A.1}$$

where Ψ_A and Ψ_B are the wave functions for isolated molecules, A and B. In the TCEHP method Ψ_3 can be rewritten as

$$\Psi_3 = B_1\Psi(\alpha \rightarrow \mu) + B_2\Psi(\beta \rightarrow \mu) \tag{A.2}$$

where $\Psi(\alpha \rightarrow \mu)$ is defined in (1), but the molecular orbitals, $\{\phi_1 \ldots \phi_\alpha \ldots \phi_\beta \ldots \phi_m \phi_\mu \phi_\nu\}$ are not orthogonalized ($2m$ = the number of electrons). E_3 can be calculated in the following procedure:

1) Transform the occupied orbital set $\{\phi_1 \ldots \phi_m\}$ except for ϕ_α, ϕ_β, ϕ_μ, and ϕ_ν to the orthonormalized orbital set $\{\phi'_1 \ldots \phi'_{m-2}\}$.
2) Orthogonalize ϕ_α, ϕ_β, ϕ_μ, and ϕ_ν to the orbitals $\{\phi'_1 \ldots \phi'_{m-2}\}$.

$$|\phi'_\zeta\rangle = n_\zeta(1 - \Sigma_{j=1}^{m-2}|\phi'_j\rangle\langle\phi'_j|)|\phi_\zeta\rangle, \qquad \zeta = \alpha, \beta, \mu \text{ and } \nu \tag{A.3}$$

that is

$$|\phi_\zeta\rangle = n_\zeta^{-1}|\phi'_\zeta\rangle + \Sigma_{j=1}^{m-2}|\phi'_j\rangle\langle\phi'_j|\phi_\zeta\rangle. \tag{A.4}$$

After transformations 1) and 2), the wave functions $\Psi(\alpha \to \mu)$ and $\Psi(\beta \to \nu)$ can be written in terms of the new orbitals as

$$\begin{aligned}\Psi(\alpha \to \mu) &= n_0 n_\beta^{-2} n_\alpha^{-1} n_\mu^{-1} \Psi'(\alpha' \to \mu') \\ \Psi(\beta \to \nu) &= n_0 n_\alpha^{-2} n_\beta^{-1} n_\nu^{-1} \Psi'(\beta' \to \nu').\end{aligned} \tag{A.5}$$

3) Orthogonalize ϕ'_α, ϕ'_β, ϕ'_μ, and ϕ'_ν to each other successively by the Schmidt method to obtain the new set (ϕ''_α, ϕ''_β, ϕ''_μ, and ϕ''_ν). The single-primed orbitals are written in terms of the double-primed orbitals:

$$\begin{aligned}\phi'_\alpha &= \phi''_\alpha \\ \phi'_\beta &= S(\beta'\alpha'')\phi''_\alpha + S(\beta'\beta'')\phi''_\beta \\ \phi'_\mu &= S(\mu'\alpha'')\phi''_\alpha + S(\mu'\beta'')\phi''_\beta + S(\mu'\mu'')\phi''_\mu \\ \phi'_\nu &= S(\nu'\alpha'')\phi''_\alpha + S(\nu'\beta'')\phi''_\beta + S(\nu'\mu'')\phi''_\mu + S(\nu'\nu'')\phi''_\nu\end{aligned} \tag{A.6}$$

where $S(\zeta'\eta'') = \langle\phi'_\zeta|\phi''_\eta\rangle$. Now the wave functions are expressed in terms of the orthonormalized orbitals $\{\phi'_1 \ldots \phi'_{m-2}\}$ and $\{\phi''_\alpha, \phi''_\beta, \phi''_\mu, \phi''_\nu\}$;

$$\begin{aligned}\Psi(\alpha \to \mu) &= n_0 n_\beta^{-2} n_\alpha^{-1} n_\mu^{-1} [C_0 \Phi''_{\mathrm{cl}} + C_1 \Psi''(\alpha'' \to \mu'') + C_2 \Psi''(\beta'' \to \mu'')] \\ \Psi(\beta \to \nu) &= n_0 n_\alpha^{-2} n_\beta^{-1} n_\nu^{-1} [D_0 \Phi''_{\mathrm{cl}} + D_1 \Psi''(\beta'' \to \mu'') + D_2 \Psi''(\beta'' \to \nu'')]\end{aligned} \tag{A.7}$$

where

$$C_0 = \begin{cases} \sqrt{2}S(\beta'\beta'')[S(\beta'\beta'')S(\mu'\alpha'') - S(\beta'\alpha'')S(\mu'\beta'')] & \text{for singlet} \\ 0 & \text{for triplet} \end{cases}$$

$$C_1 = S(\beta'\beta'')S(\mu'\mu''), \qquad C_2 = -S(\mu'\mu'')S(\beta'\alpha'')S(\beta'\beta'')$$

$$D_0 = \begin{cases} \sqrt{2}S(\beta'\beta'')S(\nu'\beta'') & \text{for singlet} \\ 0 & \text{for triplet} \end{cases}$$

$$D_1 = S(\beta'\beta'')S(\nu'\mu''), \qquad D_2 = S(\beta'\beta'')S(\nu'\nu'')$$

and n_0 is an appropriate normalization constant. In (A.7), Ψ''_{cl} is a closed shell wave function of $\{\phi'_1 \ldots \phi'_{m-2}\phi''_\alpha\phi''_\beta\}$. Now, since Ψ_3 is written in a linear combination of Ψ''_{cl}, $\Psi''(\alpha'' \to \mu'')$, $\Psi''(\beta'' \to \mu'')$ and $\Psi''(\beta'' \to \nu'')$, in which the MO's are orthonormalized, E_3 can easily be evaluated.

References

1. a) Morokuma, K.: J. Chem. Phys. **55**, 1236 (1971). b) Morokuma, K., Pederson, L.: **48**, 3275 (1968); c) Morokuma, K., Winick, J. R.: **52**, 1301 (1970)
2. Kollman, P. A., Allen, L. C.: Chem. Rev. **72**, 283 (1972), and references therein

3. Morokuma, K., Iwata, S., Lathan, W. A.: The world of quantum chemistry, Daudel, R., Pullman, B. Eds., pp. 277–316. Dordrecht, Holland: Reidel 1974
4. a) Iwata S., Morokuma, K.: Chem. Phys. Letters **19**, 94 (1973); b) Iwata, S., Morokuma, K.: J. Am. Chem. Soc. **95**, 7563 (1973); corrections: J. Am. Chem. Soc. **97**, 4786 (1975)
5. Iwata, S., Morokuma, K.: J. Am. Chem. Soc. 97, 966 (1975)
6. Iwata, S., Isaacson, A. D., Morokuma, K.: to be published
7. Morokuma, K., Iwata, S.: Chem. Phys. Letters **16**, 192 (1972)
8. Iwata, S., Morokuma, K.: Theoret. Chim. Acta (Berl.) **33**, 285 (1974)
9. a) Rein, R., Harris, F. E.: J. Chem. Phys. **41**, 3393 (1964); b) Rein, R., Harris, F. E.: J. Chem. Phys. **43**, 4415 (1965)
10. Clementi, E., Mehl, J., von Niessen, W.: J. Chem. Phys. **54**, 508 (1971)
11. Mataga, N., Kubota, T.: Molecular interactions and electronic spectra. New York: Marcel Dekker 1970
12. Karle, G., Brockway, L. O.: J. Am. Chem. Soc. **66**, 574 (1944)
13. Hehre, W. J., Stewart, R. F., Pople, J. A.: J. Chem. Phys. **51**, 2657 (1969)
14. Lathan, W. A., Morokuma, K.: J. Am. Chem. Soc. 97, 3615 (1975)
15. Hirschfelder, J. O., Curtis, C. E., Bird, R. B.: Theory of gases and liquids. New York: Wiley 1964
16. Iwata, S.: to be published
17. Kitaura, K., Morokuma, K.: Intern. J. Quantum Chem. **10**, 325 (1976)
18. Brundle, C. R., Turner, D. W., Robin, M. B., Basch, H.: Chem. Phys. Letters 3, 292 (1969)
19. Thomas, R. K.: Proc. Roy. Soc. A331, 249 (1972)
20. Brundle, C. R., Robin, M. B., Jones, G. R.: J. Chem. Phys. **52**, 3383 (1970)
21. Barnes, E. E., Simpson, W. T.: J. Chem. Phys. **39**, 670 (1963)
22. Morokuma, K., Konishi, H.: J. Chem. Phys. **55**, 402 (1971)
23. Schaefer III, H. F.: The electronic structure of atoms and molecules, p. 338 and p. 352. Reading, Massachusetts: Addison-Wesley 1972
24. a) Iwata, S., Freed, K. F.: J. Chem. Phys. **61**, 1500 (1974); b) Mulliken, R. S.: Chem. Phys. Letters **25**, 305 (1974); c) Whitten, J. L.: J. Chem. Phys. **56**, 5485 (1972)
25. Iwata, S.: to be published

Received July 30, 1976